Hydrodynamics of pair-annihilating disclination lines in nematic liquid crystals

D. Svenšek* and S. Žumer
Oddelek za Fiziko, Fakulteta za Matematiko in Fiziko, Univerza v Ljubljani, Jadranska 19, SI-1000 Ljubljana, Slovenia
(Received 24 April 2002; published 23 August 2002)

The pair annihilation of straight line defects with strength $\pm 1/2$ in bulk nematic systems is studied numerically, considering a full coupling of orientational degrees of freedom and hydrodynamics. This work is based on the generalization of the Ericksen-Leslie theory to the tensor order parameter as proposed by Qian and Sheng [T. Qian and P. Sheng, Phys. Rev. E **58**, 7475 (1998)]. The approach is particularly suited for the late stages of the annihilation process. It is confirmed that the $+1/2$ disclination line moves considerably faster than the $-1/2$ one (e.g., twice as fast) due to the hydrodynamic flow. Symmetries of the important stress tensor terms upon inverting the sign of the winding number and performing a homogeneous in-plane rotation of the Q-tensor eigensystem are discussed. The stress tensor terms that dominantly contribute to the advective flow and to the flow asymmetry are identified.

DOI: 10.1103/PhysRevE.66.021712 PACS number(s): 61.30.Jf, 61.30.Dk, 61.30.Gd, 47.15.Gf

I. INTRODUCTION

The research of defects in order parameter fields corresponding to various condensed matter systems is driven by many aspects of motivation. Defects can be readily observed, either directly (e.g., by optical methods) or through other physical properties of the system, which are crucially modified in the presence of defects. In many cases of application defect-free structures are required, while in the others (e.g., in some liquid crystal displays) structures containing defects might be essential. In the latter case, one must know something about static or dynamic properties of defects. Theoretically, defects offer a rich playground for mathematically oriented excursions. Their topological properties can be very interesting and nontrivial, if only the order parameter has enough degrees of freedom. Defects play a decisive role in any phase transition, since in the late stages the ordering is governed exclusively by the dynamics of the defects created at the transition. An important part of motivation arises from the universality of defects, i.e., they can occur in any system with a rich enough order parameter. Their major properties are independent of the underlying physics, determined solely by symmetries and dimensionalities of the order parameter, the defect and the system. Lately the aim towards the exploitation of this universality has been experienced in the area, motivating the research of laboratory-friendly condensed matter systems such as liquid crystals in order to yield knowledge in completely different realms of physics (e.g., the physics of the universe, elementary particles, and fields) [1–3].

In order to study the statics or dynamics of defects in nematic liquid crystals, the full tensorial description of the nematic ordering must be considered. If one wants to include hydrodynamic effects, normally described by the Ericksen-Leslie theory [4,5], a generalization of the latter is required to describe the coupling of the tensorial dynamics and the flow [6–8]. The director description is not adequate for the treatment of defects, in particular, it fails when studying their dynamic properties. One might expect to remedy the problem by allowing a variation of the degree of order. It turns out, however, that in the defect center the equations so obtained are ill conditioned numerically and incapable of accurately describing the hydrodynamic part of the problem.

To our knowledge, there have been only a few papers published on defect dynamics including hydrodynamics. The Effect of hydrodynamic flow on kinetics of nematic-isotropic transition has been studied by Fukuda [9], a similar topic, however with a different method—the lattice Boltzmann algorithm, has been studied by Denniston *et al.* [10]. Recently a paper on the hydrodynamics of topological defects was published by Tóth, Denniston, and Yeomans [11]. They studied the effect of back flow and elastic anisotropy on the pair annihilation of straight line defects with strengths $\pm 1/2$, again using the lattice Boltzmann algorithm. Their treatment, however, is not based on the Ericksen-Leslie theory and involves only two viscous coefficients.

The aim of our paper is to present the solution to the pair annihilation of straight disclination lines with strengths $\pm 1/2$, starting from the generalization of the standard Ericksen-Leslie (EL) theory to the tensor order parameter [8]. We consider an unconfined bulk system. The generalized theory involves the same number of viscous parameters as the EL theory, expressed as simple linear combinations of the Leslie viscosity coefficients. Since the Leslie coefficients represent the standard way of materializing the viscous dissipation in nematics and enough data is available for many compounds, at least on the α_2 and α_3, we believe, that the present work will be appreciated in the field.

An alternative (complementary) method to the lattice Boltzmann algorithm used in Ref. [10] is to be demonstrated, based on solving partial differential equations for the order parameter and the velocity field. Symmetry properties of the stress tensor with respect to changing the sign of the winding number will be discussed, resulting in a simple yet accurate identification of stress tensor terms, responsible for the observed flow asymmetry and the acceleration of the annihilation process. Further, it is to be shown that the hydrodynamic effect depends on the director phase angle, i.e., unlike the

*Corresponding author. FAX: +386 1 2517281. Email address: daniel@fiz.uni-lj.si

order parameter dynamics in the case of elastic isotropy considered here, it is not invariant under the homogeneous rotation of directors. Again the corresponding stress tensor term will be pointed out.

It should be stressed that although the tensorial approach works very well at small defect separations, the passage to 1 μm length scales that can be resolved experimentally is hindered by enormous computational complexity of the problem and the large (several orders of magnitude) ratio of the defect separation to the size of the defect core.

II. DYNAMIC EQUATIONS

The starting point is the bulk free energy density expression in terms of Q ([12], p. 156),

$$f=\phi(\mathsf{Q})+\tfrac{1}{2}L\,\partial_i\mathsf{Q}_{jk}\partial_i\mathsf{Q}_{jk}, \tag{1}$$

where the homogeneous part is given by

$$\phi(\mathsf{Q})=\tfrac{1}{2}A\mathsf{Q}_{ij}\mathsf{Q}_{ji}+\tfrac{1}{3}B\mathsf{Q}_{ij}\mathsf{Q}_{jk}\mathsf{Q}_{ki}+\tfrac{1}{4}C(\mathsf{Q}_{ij}\mathsf{Q}_{ji})^2. \tag{2}$$

It was taken into account that $C_1(\mathsf{Q}_{ij}\mathsf{Q}_{ji})^2+C_2\mathsf{Q}_{ij}\mathsf{Q}_{jk}\mathsf{Q}_{kl}\mathsf{Q}_{li}=(C_1+1/2C_2)(\mathsf{Q}_{ij}\mathsf{Q}_{ji})^2$ and a new constant $C=C_1+C_2/2$ was introduced. In the elastic part of Eq. (1), only the term with $L_1\equiv L$ is retained, resulting in isotropic elasticity. Terms of third order in Q are needed to reach the splay-bend elastic anisotropy [13], the effects of which have been studied in Ref. [11].

Requiring the Q tensor to be traceless and symmetric, the Euler-Lagrange equation for the functional

$$F=\int dV[\,f(\mathsf{Q},\nabla\mathsf{Q})-\lambda\mathsf{Q}_{ii}-\lambda_i\epsilon_{ijk}\mathsf{Q}_{jk}] \tag{3}$$

gives the homogeneous and elastic part of the generalized force on the tensor order parameter Q,

$$\mathsf{h}^{he}_{ij}=L\,\partial_k^2\mathsf{Q}_{ij}-\frac{\partial\phi}{\partial\mathsf{Q}_{ij}}+\lambda\,\delta_{ij}+\lambda_k\epsilon_{kij}\,. \tag{4}$$

The Lagrange-multiplier terms merely state that the isotropic and antisymmetric components of Eq. (4) are not specified and have to be determined by the constraints, i.e., the isotropic and antisymmetric parts must be subtracted from the force h^{he}_{ij}. The elastic stress tensor is obtained in a standard manner as

$$\sigma^e_{ij}=-\frac{\partial f}{\partial(\partial_i\mathsf{Q}_{kl})}\partial_j\mathsf{Q}_{kl}\,. \tag{5}$$

The viscous stress tensor and the viscous generalized force on the Q tensor are given by a tensorial generalization of the Ericksen-Leslie theory [8],

$$\sigma^v_{ij}=\beta_1\mathsf{Q}_{ij}\mathsf{Q}_{kl}\mathsf{A}_{kl}+\beta_4\mathsf{A}_{ij}+\beta_5\mathsf{Q}_{ik}\mathsf{A}_{kj}+\beta_6\mathsf{Q}_{jk}\mathsf{A}_{ki}+\tfrac{1}{2}\mu_2\mathsf{N}_{ij}-\mu_1\mathsf{Q}_{ik}\mathsf{N}_{kj}+\mu_1\mathsf{Q}_{jk}\mathsf{N}_{ki}\,, \tag{6}$$

$$-\mathsf{h}^v_{ij}=\frac{1}{2}\mu_2\mathsf{A}_{ij}+\mu_1\mathsf{N}_{ij}\,, \tag{7}$$

where

$$\mathsf{N}_{ij}=\frac{d\mathsf{Q}_{ij}}{dt}+\mathsf{W}_{ik}\mathsf{Q}_{kj}-\mathsf{Q}_{ik}\mathsf{W}_{kj}\,, \tag{8}$$

with the material time derivative $d\mathsf{Q}_{ij}/dt=\partial\mathsf{Q}_{ij}/\partial t+(\mathbf{v}\cdot\nabla)\mathsf{Q}_{ij}$ and the symmetric and antisymmetric parts of the velocity gradient $\mathsf{A}_{ij}=\frac{1}{2}(\partial_i v_j+\partial_j v_i)$ and $\mathsf{W}_{ij}=\frac{1}{2}(\partial_i v_j-\partial_j v_i)$. Only those terms have been included that in the uniaxial limit with a constant degree of order reduce to the standard Leslie viscous terms α_i. Thus, the viscous coefficients in Eqs. (6) and (7), linked by the relation $\mu_2=\beta_6-\beta_5$, can be expressed in terms of the Leslie coefficients and the constant value of the scalar order parameter [8].

Finally, the equation of motion for the Q tensor is the symmetric traceless part of

$$\mathsf{h}^{he}+\mathsf{h}^v=0, \tag{9}$$

with the constraints

$$\mathsf{Q}_{ii}=0,\quad \epsilon_{ijk}\mathsf{Q}_{jk}=0. \tag{10}$$

The generalized Navier-Stokes equation within the low-Reynolds-number approximation [omitting the nonlinear advective derivative term $(\mathbf{v}\cdot\boldsymbol{\nabla})\mathbf{v}$], regularly made for the order parameter elasticity driven dynamics in liquid crystals [14,15], reads

$$\rho\frac{\partial v_i}{\partial t}=-\partial_i p+\partial_j(\sigma^v_{ji}+\sigma^e_{ji}), \tag{11}$$

with the density ρ and the viscous and elastic stress tensors given in Eqs. (6) and (5). Usually, also the steadiness approximation is made, omitting the time derivative term [14,15]. The pressure field p must be such that the incompressibility condition

$$\partial_i v_i=0 \tag{12}$$

is satisfied. Equation (9) and the stationary version of Eq. (11) can both be put to a dimensionless form by introducing a characteristic length, e.g., the correlation length, a couple of nanometers usually,

$$\xi=\sqrt{\frac{3}{2}\frac{L}{\phi''|_{S_0}}}, \tag{13}$$

with $\mathsf{Q}_{ij}=S/2(3n_in_j-\delta_{ij})$ and $\phi''|_{S_0}$ the equilibrium value of the second derivative of Eq. (2) with respect to the scalar order parameter S, and a characteristic time

$$\tau=\gamma_1\xi^2/K=\mu_1\xi^2/L, \tag{14}$$

where γ_1 is the director rotational viscosity and K is the director elastic constant. The time τ is the characteristic relaxation time of the order parameter deformation on the length scale of ξ, which is typically tens of nanoseconds. In the following, dimensionless quantities will be used, i.e., $r\leftarrow r/\xi$ for length, $t\leftarrow t/\tau$ for time and $v\leftarrow v\,\tau/\xi$ for the ve-

locity. After doing so, the material parameters enter the equations only through combinations given in Eqs. (17) and (18).

Let us estimate the Reynolds number and the unsteadiness parameter of the flow, i.e., the ratio of characteristic dynamic times of the flow field and the order parameter field. The estimate differs from those made in Refs. [14,15], in that now there is no simple relation between the characteristic deformation length (13) of the order parameter field and its relaxation time. Instead, one can empirically identify the latter with the annihilation time. This yields the Reynolds number and the unsteadiness parameter of

$$\mathrm{Re}=\frac{\rho K}{\gamma_1^2}\frac{R_0^2}{t}\approx 10^{-6}\times\frac{R_0^2}{t}, \tag{15}$$

where R_0^2 is the initial defect separation and t is the annihilation time. The isotropic viscosity was put equal to γ_1 for brevity. The value of R_0^2/t, obtained empirically, is of the order of a few units. What is more, following the phenomenological equation of motion given by Pleiner [16,17,11],

$$\frac{dR}{dt}\propto\frac{1}{R}\ln^{-1}\left(\frac{R}{\xi'}\right), \tag{16}$$

where $R(t)$ is the actual defect separation and ξ' scales with ξ, the value of R_0^2/t exhibits only a weak logarithmic dependence on R. Thus, for large enough defect separations compared with ξ, the empirical estimate is quite general in validity. In conclusion, the Reynolds number and the unsteadiness parameter are tiny indeed, so that in Eq. (11) both the advective and partial time derivatives can be omitted.

III. NUMERICAL APPROACH

The coupled partial differential equations (9) and (11) are solved using finite difference discretization. The outline of the method is as follows. At a given tensor field and its time derivative, the linear generalized Navier-Stokes equation (11) is explicitly iterated in time until the velocity field becomes stationary to a good enough accuracy. After that, knowing the velocity field, the tensor equation (9) is explicitly iterated in time to yield the new tensor field. Then the velocity is updated again, and so forth. The variables are discretized on a staggered grid ([18], p. 331) in order to prevent the occurrence of the well-known oscillatory pressure solution. Hereby the tensor components are discretized in the central (pressure) points of the staggered grid. The incompressibility condition is satisfied in a standard way by solving a Poisson equation for pressure corrections ([18], p. 340) at every velocity iteration step via a simultaneous overrelaxation method ([19], p. 655). At the boundaries, normal pressure correction derivatives are specified in order to meet the incompressibility condition there. The calculations were done on an inhomogeneous square mesh, consisting of a fine mesh of 160×160 points in the center containing both defects, and a coarser inhomogeneous grid with increasing spacing around it to yield the total of 280×280 points. The position of the defects was determined by finding a local minimum of the trace $\mathsf{Q}_{ij}\mathsf{Q}_{ij}$.

The velocity was set to zero at the boundary. In order to meet the situation present in a bulk system, the defect separation was small compared to the size of the computational area (the ratio of the two was 3/20) and the derivatives of the order parameter normal to the boundary were set to zero. Initially, the Q tensor was set to $\mathsf{Q}_{ij}=1/2(3n_in_j-\delta_{ij})$, where $\mathbf{n}=(\cos\phi,\sin\phi)$ and $\phi=\Sigma_{k=1}^{2}m_k\arctan[(y-y_k)/(x-x_k)]$, which is the one elastic constant equilibrium director configuration with two defects of strength m_k positioned at (x_k,y_k). Afterwards, enough computing steps without the hydrodynamics were performed to first establish the full tensorial configuration. The initial defect separation was above 70 correlation lengths, Eq. (13), in order to reach the far regime of motion, where the defects are well isolated. As one realizes, there are three length scales in the system, which should be well enough separated: the correlation length and the defect spacing as the relevant physical scales, plus the container size as the technical one.

The viscosity coefficients in Eqs. (6) and (7) were obtained from the standard Leslie coefficients corresponding to MBBA (4-methoxybenzyliden-4′-butylanilin) ([20], p. 231) as described in Ref. [8]. Numerical values of the relevant ratios are

$$\mu_2/\mu_1\approx-1.92,\quad \beta_1/\mu_1\approx0.17,\quad \beta_4/\mu_1\approx1.99,$$
$$\beta_5/\mu_1\approx0.70,\quad \beta_6/\mu_1\approx-0.79. \tag{17}$$

The Landau coefficients A,B,C and the elastic constant L in Eqs. (1) and (2) were taken from Ref. [21]. Numerical values of the relevant ratios are

$$A\xi^2/L\approx-0.064,\quad B\xi^2/L\approx-1.57,\quad C\xi^2/L\approx1.29, \tag{18}$$

with the correlation length, Eq. (13), $\xi\approx2.11$ nm. The characteristic time, Eq. (14), $\tau\approx32.6$ ns completes the set of material parameters.

IV. RESULTS AND DISCUSSION

The results for the pair annihilation of $\pm1/2$ defects (Fig. 1) are presented in Fig. 2. It should be pointed out that due to the high computational complexity of the problem and the broad range of length scales involved, only defect separations of less than 1 μm and annihilation times of less than 1 ms can be reached. This means that for the time being there still exists a large gap between numeric capabilities and possible experimental observations.

In Fig. 2 one notices two distinct features: due to the hydrodynamic flow the annihilation is faster and asymmetric. Figure 3 shows that it is particularly the $+1/2$ defect whose motion is affected by the flow. Also clearly demonstrated by Fig. 3 (see also Figs. 5 and 6) is the nonmonotonic behavior of the defect velocities at early stages of the annihilation ([3], p. 58). It is a consequence of starting with the equilibrium configuration of fixed defects rather than with a dynamic one, which is being approached by the system in the course of annihilation. Since our simulations represent only the very

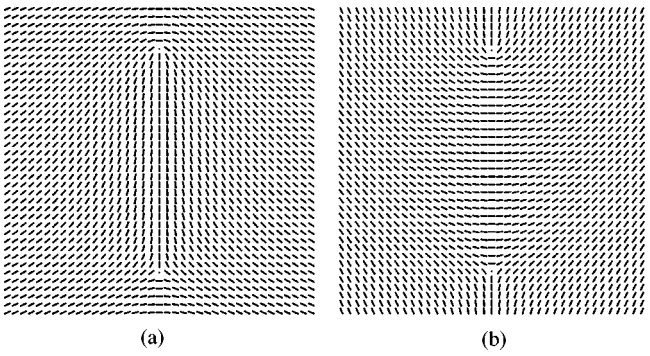

FIG. 1. A schematic representation of a pair of $\pm 1/2$ defect lines: the eigenvectors corresponding to the largest absolute eigenvalue of Q (directors) are depicted in the cross-sectional plane, perpendicular to the disclination lines. Two isomorphs (a) and (b) are shown, differing only in a homogeneous rotation of the directors. For clarity, the number of mesh points has been reduced by a factor of 4 in each dimension and the correlation length has been increased by a factor of 2 (only the central homogeneous region of the mesh is shown).

late stage of an actual annihilation process, this nonmonotonic behavior should be viewed as an unphysical artifact of the initial condition. In a separate work to follow, we show that it can be eliminated by starting with a proper dynamic configuration, even without throwing away computational resources for simulating larger defect separations.

First, let us concentrate on qualitative features of the flow-driving mechanism by inspecting the stress tensors (5) and (6). One is tempted to explain the easily perceived characteristic of the flow field [Fig. 4(a)]: due to advection the $+1/2$ defect is sped up, while the flow is much weaker around the $-1/2$ defect.

As hinted by the previous work [14] and verified numerically, the ''passive'' β_1, β_5, and β_6 terms in the viscous stress tensor (6) (or their counterparts in the standard Ericksen-Leslie theory, α_1, α_5, and α_6), describing the dependence of the fluid viscosity on the order parameter, give

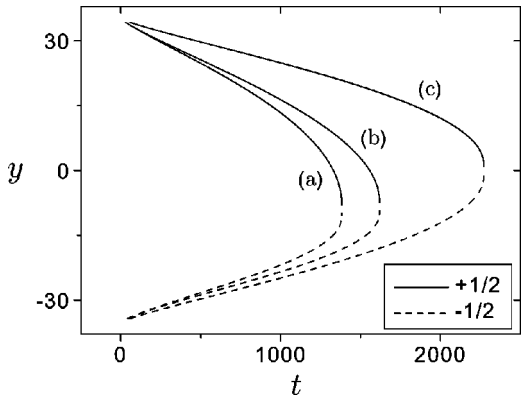

FIG. 2. Position of the defects as a function of time, measured from the initial middle point between the defects. Three situations are displayed: the two isomorphs (a) and (b) (see Fig. 1) and the case without the flow (c), where the isomorphs become degenerate. We remember that length is measured relative to $\xi \approx 2.1$ nm, and time is measured relative to $\tau \approx 33$ ns.

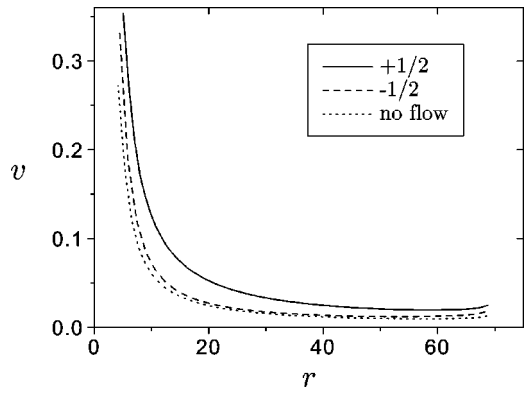

FIG. 3. Velocity of the defects as a function of the interdefect distance [isomorph (a)]. For comparison, the same is shown for the case without the hydrodynamic flow. The velocity of the $+1/2$ defect is strongly increased by the flow. Note the nonmonotonic behavior at early stages of the process, where the initial equilibrium Q-tensor configuration is adapting to a dynamic one ([3], p. 58). The distance and the velocity are measured relative to $\xi \approx 2.1$ nm and $\xi/\tau \approx 65$ nm/μs, respectively.

only minor quantititative effects. Therefore one can ignore them in striving to gain a qualitative picture. On the other hand, the remaining μ_1 and μ_2 terms, which contain the order parameter time derivative $\dot{\mathsf{Q}}$, and also the elastic stress tensor (5), represent the source driving the flow and therefore have to be analyzed carefully.

A. The flow asymmetry

At this stage, we are interested only in symmetries, i.e., the behavior of the stress tensor terms considered upon changing the order parameter field locally as to transform the $+1/2$ and $-1/2$ defects one into the other. In one elastic constant approximation, this can be achieved by mirroring the Q tensor on the axis joining the defects (the y axis, Fig. 1) [10]: $\mathsf{Q}_{xy} \rightarrow -\mathsf{Q}_{xy}$, since the free energy density (1) is left unchanged by this procedure. Any stress tensor terms, invariant with respect to this transformation, treat both defects equally, and clearly do not contribute to the flow asymmetry. On the other hand, any noninvariant terms must be identified as the flow symmetry-breaking components.

By definition (5) the elastic stress tensor is invariant, which is a direct consequence of the elastic isotropy. As a result, the flow field is the same for both defects [Fig. 4(b)]. In addition, its direction is such as to reduce the interdefect separation and thereby the free energy of the system. This follows immediately from the definition of any stress tensor.

The viscous terms will be analyzed for the case $\mathbf{v}=\mathbf{0}$, i.e., only the driving ($\dot{\mathsf{Q}}$-dependent) part in Eq. (8) will be considered. The μ_2 term has no definite symmetry for some of its components transform symmetrically and some antisymmetrically. At the defect spots the flow driven by this term is rather weak compared to the contribution from the other terms in question, because $\dot{\mathsf{Q}}$ is extremal there yielding a vanishing divergence. Hence, the μ_2 term does not give a dominant contribution to the advective motion of the defects.

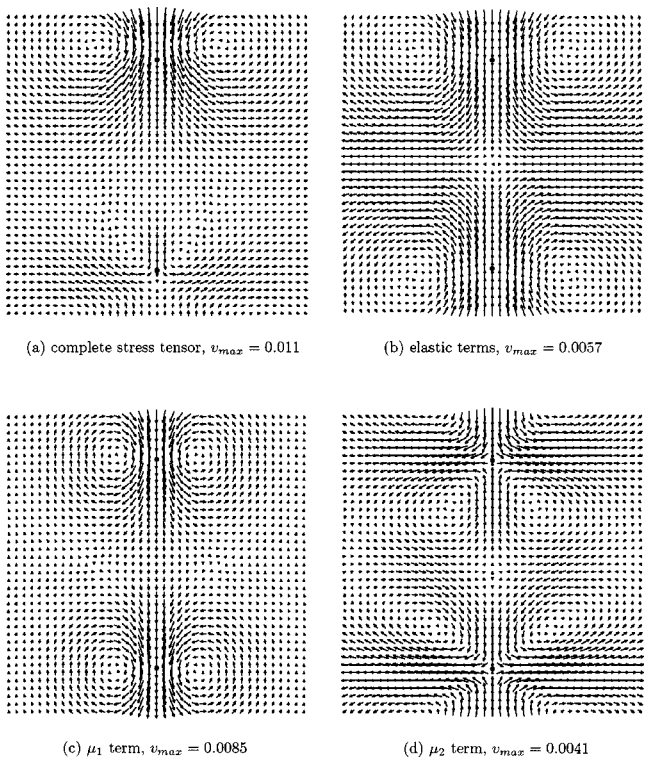

FIG. 4. Flow fields resulting from different driving stress tensor terms: (a) the complete stress tensor, (b) elastic stress, (c) the μ_1 viscous term, and (d) the μ_2 viscous term. In all cases the isotropic β_4 viscous term is also included. For clarity, the number of mesh points has been reduced by a factor of 4 in each dimension; only the central homogeneous region of the mesh is shown. The approximate positions of defects are marked with circles; the radius of the defect core is roughly four grid points. The maximum velocity magnitude v_{max} corresponding to the longest velocity vector is given for each flow field (relative to ξ/τ).

On the other hand, the μ_1 term is fully antisymmetric with respect to the transformation, yielding exactly the opposite flow for the $-1/2$ defect as compared with that near the $+1/2$ defect [Fig. 4(c)]. One notices that the flow is the strongest at the defect positions in this case. Thus, due to advection this term alone can give rise to the flow asymmetry observed. One can verify by inspecting Eqs. (6) and (7) that the relative magnitude of this antisymmetric contribution to the advective derivative term $(\mathbf{v}\cdot\boldsymbol{\nabla})\mathrm{Q}$ in Eq. (9) is approximately proportional to μ_1, provided that all other material parameters are kept fixed. On the other hand, scaling all viscosities equally with respect to the elastic constant leaves the dynamics unchanged completely and merely alters the characteristic time (14), a statement based purely on dimensional grounds (see Sec. II).

In addition to the flow asymmetry, the annihilation process is also significantly sped up when compared to the annihilation without the flow. Following the previous discussion, this effect is caused mostly by the elastic stress driven flow. Thus, the annihilation dynamics offers a nice example showing the importance of the elastic stress in liquid crystals (LC), which is usually considered less significant, e.g., in LC cells. Additionally, the elastic and μ_1 viscous terms act in concord near the $+1/2$ defect, whereas for the $-1/2$ defect they combine destructively. This explains the different velocity magnitudes in the vicinity of the defects [Fig. 4(a)].

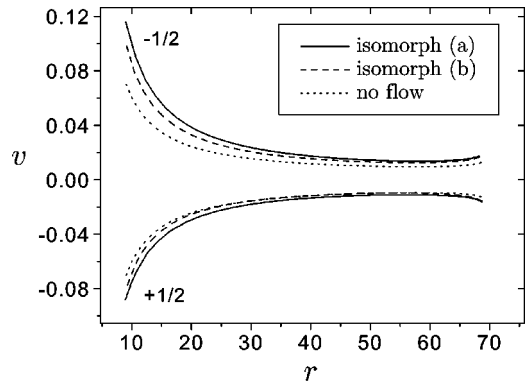

FIG. 5. Velocity of the defects without the contribution of advection as a function of the interdefect distance. Without the hydrodynamic flow, both defects move symmetrically. Note that the part of the velocity coming from the order parameter dynamics is larger for the $-1/2$ defect. Also note the difference between the isomorphs originating from the different coupling to flow and different flow field itself, both of which are due to the μ_2 viscous term.

B. Reorientation-driven defect motion vs flow advection

It is also of one's interest to quantify the ratio of defect motion due to advection as opposed to the motion propelled by the order parameter dynamics. Figures 5 and 6 show that the velocities in question are quite comparable in magnitude. Once again this reflects the importance of the flow in defect dynamics as compared with the limited perturbing effects it normally has, e.g., in LC cells [14]. Furthermore, one must realize that also a secondary flow effect besides advection is important, namely, the influence of the flow on the order parameter dynamics. It is clear from Fig. 5 that the order parameter dynamics itself is faster because of the coupling to the flow. Comparing Figs. 5 and 6 one can state that the contribution of this coupling to the flow asymmetry is less important than that of the advection, whereas its accelerating effect is just as important.

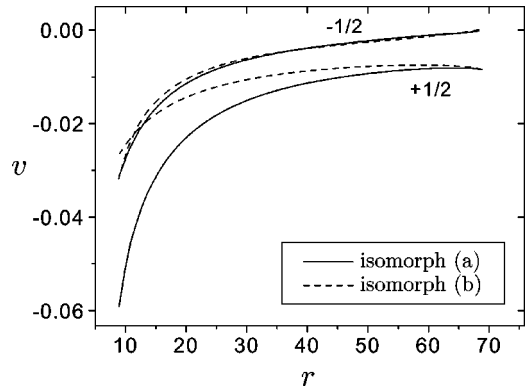

FIG. 6. The advective contribution to the velocity of the defects for the two isomorphic cases. The surprisingly large difference between the velocities of the $+1/2$ defect is mainly due to the μ_2 viscous term. At small separations not shown, the motion driven by the order parameter dynamics (Fig. 5) becomes dominant.

C. Influence of the director orientation angle on the flow

In one elastic constant approximation, the free energy density (1) and thus the order parameter dynamics are invariant with respect to a homogeneous rotation of the eigensystem of the Q tensor in every space point. Consequently, defect pairs, differing only in this constant phase angle of director rotation—*isomorphs* (Fig. 1), behave exactly in the same way (e.g., for the case of a $+1$ defect such isomorphs are the radial and tangential defects, as well as any other form between the two). With the flow present, however, this symmetry is broken (Fig. 2). It is quite instructive to study the dependence of the important stress tensor terms upon such a rotation. Besides the elastic term (5), the μ_1 pair of terms is also left unchanged by the rotation. This is why the effect of advection should be roughly similar for all isomorphs. It is worth mentioning that also the influence of the flow on the Q tensor given by the μ_1 term in Eq. (7) is not affected by the rotation.

On the other hand, the μ_2 stress tensor term is not invariant. One can see in Fig. 6 that it introduces significant differences even as far as the advection of the defects is concerned. For general isomorphs the μ_2 term yields a flow field lacking the symmetry of reflection on the axis joining the defects. Additionally, the μ_2 term in the viscous force (7) is different for different isomorphs. It is due both to the different coupling of the flow to the order parameter dynamics and to the differences in advection that the isomorphs are not equivalent dynamically. As verified numerically, the β_1, β_5, and β_6 terms again bring only a very small difference.

V. CONCLUSION

We have studied the attraction and annihilation of straight line defects with charge $\pm 1/2$ in bulk nematics. Our approach is based on the tensorial generalization of the standard Ericksen-Leslie theory for nematic liquid crystals and thus in direct contact with the concepts well accepted and accustomed to in this area of research. It has been shown that due to the hydrodynamic flow, the annihilation is faster and asymmetric. Further, we have identified the governing stress tensor terms: the μ_1 and μ_2 viscous terms and the elastic stress. Symmetries of the terms upon inverting the sign of the winding number and performing a homogeneous in-plane rotation of the Q-tensor eigensystem have been discussed. Both the μ_1 term and the elastic stress are invariant upon the rotation and hence identical for all isomorphs. The μ_1 term is antisymmetric with respect to changing the sign of the defects, thereby contributing dominantly to the annihilation asymmetry. On the other hand, the elastic stress is symmetric, so that it causes the annihilation process to go on faster. The only terms distinguishing between different isomorphs are the μ_2 terms in Eqs. (6) and (7) (they also distinguish between the $+1/2$ and $-1/2$ defect). Thus, one can conclude that the difference in dynamics between the isomorphs is governed by the ratio μ_2/μ_1. The remaining β_1, β_5, and β_6 terms in the viscous stress tensor (6) introduce only inferior corrections to the flow field.

One should emphasize once more that due to length scales several orders of magnitude apart and enormous computational complexity of the problem, with the present method one is unable to reach the $>1\mu$m range of interdefect distances, which can be resolved in experiments. Nevertheless, it is quite reasonable to believe that the hydrodynamic effects described in this paper, i.e., the flow asymmetry and the reduction of the annihilation time, will be present also at larger defect separations.

ACKNOWLEDGMENTS

The authors wish to express gratitude to Professor H. R. Brand for fruitful discussions. This work was supported by the Slovenian Office of Science (Program No. P0-0503-1554), the US-Slovene NSF Joint Fund (Grant No. 9815313), and the SILC TMR ERBFMRX-CT98-0209 project.

[1] W. H. Zurek, Nature (London) **317**, 505 (1985).
[2] H.-R. Trebin, Liq. Cryst. **24**, 127 (1998).
[3] L. M. Pismen, *Vortices in Nonlinear Fields* (Oxford University Press, Oxford, 1999).
[4] J. L. Ericksen, Arch. Ration. Mech. Anal. **4**, 231 (1960).
[5] F. M. Leslie, Q. J. Mech. Appl. Math. **19**, 357 (1966); Arch. Ration. Mech. Anal. **28**, 265 (1968).
[6] S. Hess, Z. Naturforsch. Teil A **31**, 1507 (1976).
[7] P. D. Olmsted and P. Goldbart, Phys. Rev. A **41**, 4578 (1990).
[8] T. Qian and P. Sheng, Phys. Rev. E **58**, 7475 (1998).
[9] J. I. Fukuda, Eur. Phys. J. B **1**, 173 (1998).
[10] C. Denniston, E. Orlandini, and J. M. Yeomans, Phys. Rev. E **64**, 021701 (2001).
[11] G. Tóth, C. Denniston, and J. M. Yeomans, Phys. Rev. Lett. **88**, 105504 (2002).
[12] *Introduction to Liquid Crystals,* edited by E. B. Priestley, P. J. Wojtowicz, and P. Sheng (Plenum Press, New York, 1974).
[13] S. Kralj and S. Žumer, Phys. Rev. A **45**, 2461 (1992).
[14] D. Svenšek and S. Žumer, Liq. Cryst. **28**, 1389 (2001).
[15] D. Svenšek and S. Žumer, Continuum Mech. Thermodyn. **14**, 231 (2002).
[16] H. Pleiner, Phys. Rev. A **37**, 3986 (1988).
[17] B. Yurke, A. N. Pargellis, T. Kovacs, and D. A. Huse, Phys. Rev. E **47**, 1525 (1993).
[18] C. A. J. Fletcher, *Computational Techniques for Fluid Dynamics* (Springer Verlag, Berlin, 1988), Vol. II.
[19] W. H. Press, B. P. Flannery, S. A. Teukolsky, and W. T. Vetterling, *Numerical Recipes* (Cambridge University Press, Cambridge, 1986).
[20] P. G. de Gennes and J. Prost, *The Physics of Liquid Crystals* (Clarendon Press, Oxford, 1995).
[21] H. J. Coles, Mol. Cryst. Liq. Cryst. **49**, 67 (1978).